JOURNAL OF MATERIALS SCIENCE 27 (1992) 2273–2278

Effects of hydrogen on the hydride transformation in Ti–24Al–11Nb alloys

P. ROZENAK*, M. DANGUR
Department of Materials Engineering, Ben-Gurion University of the Negev, Beer-Sheva 84105, Israel

The effect of hydrogen on phase transformation in Ti–24Al–11Nb alloys has been studied by means of an X-ray technique. The quantitative X-ray method is aimed at the analysis of the hydride distribution in thin surface layers comparable to the penetration depth of X-rays. In Ti–24Al–11Nb alloys cathodically charged with hydrogen, transformation of $AlTi_3$ is probably due to $AlTi_3$-H, and depends on the particular hydrogen distribution in the specimen. The fraction of $AlTi_3$-H drops from about 70% on the surface to zero at a depth of approximately 2 μm for samples which were charged for 24 h and aged for 4 h. The weight fraction of the $AlTi_3$-H hydride in the surface decreased to about 64% after a long period of ageing (7 days). Cathodic charging with hydrogen induced cracking.

1. Introduction

Considerable attention has been paid to the effect of hydrogen on the formation of hydrides and the phase stability of titanium aluminides because of their application as aircraft components [1]. Hydrogen embrittlement of titanium-based alloys, most often associated with hydride formation, is very complex. These complications arise primarily through the large variations in the hydrogen solubilities and the transport behaviour that can be developed as the result of the relative amount and distribution of the α and β phases [2, 3]. When hydrogen is originally present in an α alloy, hydride formation is often found, due to the extremely small solid solubility of hydrogen [4, 5]. Hydrogen embrittlement is the result of the presence of the brittle titanium hydride distributed through the α-phase. Very little understanding presently exists on the hydrogen interaction with the titanium-aluminides and the formation of hydride in the α-phase.

The purpose of this study is to characterize the effects of hydrogen on the $AlTi_3$ phase and hydride transformations in Ti–24Al–11Nb alloys. A quantitative X-ray method was applied to the analysis of hydride distribution in cathodically charged specimens.

2. Experimental procedure

The studies were carried out on the alloy Ti–24Al–11Nb (at %). Compositional analysis revealed a trace of iron (0.08 wt %), and low levels of oxygen (0.084 wt %) and nitrogen (0.03 wt %). The materials were forged, rolled, and solution-treated at 1150 °C for 1 h in vacuo, and cooled in argon (approximately 1 °C sec^{-1}). Afterwards they were aged at 760 °C for 1 h in vacuo, and then air-cooled. X-ray studies revealed the existence of a preferred orientation in the microstructure.

Hydrogen charging (during periods of 12 and 24 h) was performed at room temperature in a 1N H_2SO_4 solution with 0.25 g l^{-1} of $NaAsO_2$ added as a hydrogen recombination poison. A platinum electrode and current densities of 50 and 100 mA cm^{-2} were used. A Philips diffractometer was used for the X-ray diffraction study. With the Bragg–Brentano geometry, information is only obtained from the thin layer of the flat sample. The thickness $t_{0.95}$ (where $t_{0.95}$ represents the thickness at which 95% of X-rays are scattered) was calculated from the equation of the intensity of X-rays scattered by the surface layer [6]. For $AlTi_3$ 200 and 421 peaks obtained by Cu$K\alpha$ radiation, $t_{0.95}$ values are equal to 5.208 and 14.08 μm, respectively. For Co$K\alpha$ radiation the diffraction peaks of $AlTi_3$ 200 and 203, $t_{0.95}$ values are equal to 3.98 and 7.56 μm, respectively, and for $AlTi_3$ 101 and 201 peaks for Cr$K\alpha$ radiation, $t_{0.95}$ values are equal to 1.94 and 2.99 μm, respectively. The hydrogen content was determined in a Leco RH-1 and was about 1000 (wt.) p.p.m. after 24 h (50 mA cm^{-2} current density) of cathodic charging at room temperature. TEM analysis was carried out to characterize cracking formation of Ti–24Al–11Nb alloys by a Joel 200 B electron microscope operating at 150 kV. Specimens suitable for electron microscopy were prepared by the jet Tenupol polishing cell using a solution of 1 part (by volume) of perchloric acid, 6 parts n-butanol, and 10 parts of methanol at 250 K.

3. Results and discussion

The X-ray diffraction pattern obtained from an uncharged specimen agreed with those observed by Goldak and Parr [7], and revealed the existence of a hexagonal $AlTi_3$–Nb α_2 phase with lattice parameters: $a = 0.5793$ nm and $c = 0.4653$ nm. No superlattice reflections were observed; however, the reflections of the

*Permanent address: Eshel 44, OMER 84965, Israel.

0022–2461 © *1992 Chapman & Hall*

diffraction pattern show small differences that depend on composition and distortion of the hexagonal phase.

During the electrolytic charging large amounts of hydrogen are driven into the specimen. X-ray diffraction patterns of $AlTi_3$–Nb alloys, taken after various times of charging and ageing for Co-$K\alpha$ radiation are shown in Fig. 1. The $AlTi_3$ phase reflections exhibit broadening, and are shifted to smaller 2θ values, consistent with the presence of a large hydrogen concentration gradient. After severe charging (100 mA cm^{-2}) the 002 peak from the $AlTi_3$ phase has an expanded spacing of $d = 0.23511$ nm, which is about 3.0% greater than that of the original matrix (Fig. 1). Ageing after cathodic charging resulted in a number of structural changes when hydrogen outgassed from the specimen. Reflections obtained from the hydrogenated

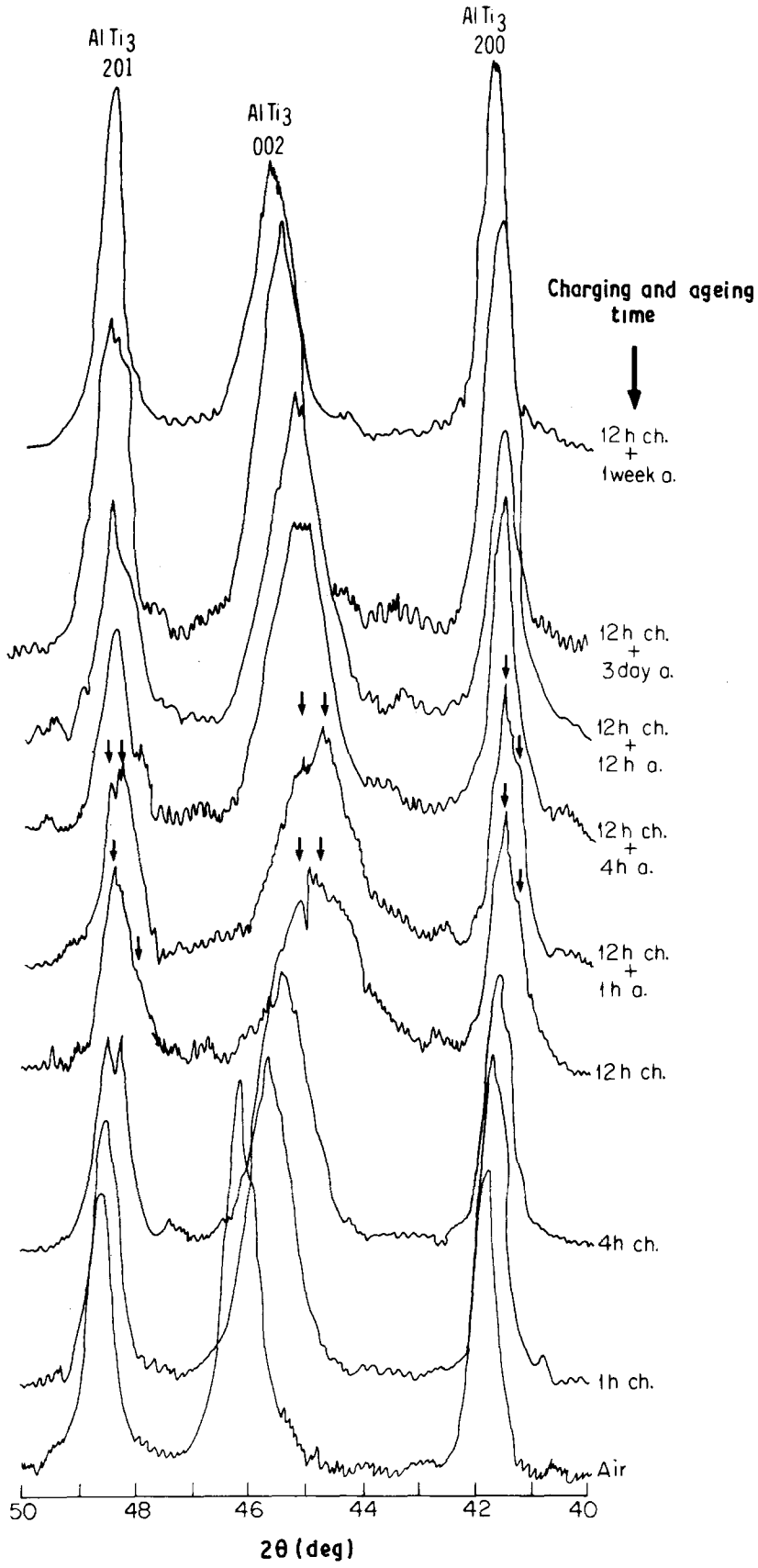

Figure 1 X-ray diffraction patterns after charging and ageing times indicated, (Co-$K\alpha$ radiation) of Ti–24Al–11Nb alloys.

$AlTi_3$ phase exhibit significant broadening, and were shifted to higher 2θ values, indicating a decrease in lattice parameter. This shift is accompanied by a decrease in peak width. On diffractograms obtained after various charging and ageing times, splitting of peaks (marked by arrows) was observed, and reflects a change in the peak profiles. The diffraction lines reflected from the hydogenated layer are superposed on those of the matrix, which are obviously increased if radiation of high $CrK\alpha$, $CoK\alpha$ and $CuK\alpha$ penetration power is utilized, suggesting that hydrogenated layers are formed close to the specimen surface (Fig. 2a to 2c). On these $CrK\alpha$ high resolution diffractograms (Fig. 2a), splitting of $AlTi_3$-H (hydride) peaks (with 1.6% expanded lattice parameter) from $AlTi_3$ matrix was observed clearly in the early stage (4 h) of ageing and (after originally 24 h of cathodic charging). Due to an overlap of $AlTi_3$-H and $AlTi_3$ peak profiles change in shape during the ageing process. Both lines slightly shifted to large 2θ angles during the ageing, indicating a recovery lattice expansion which occurred on charging (Fig. 2a). The intensity of the $AlTi_3$-H decreased, however, and those of the $AlTi_3$ increased. The intensity obtained from $AlTi_3$-H decreases with ageing time, but persists even after prolonged ageing (7 days). Diffractions, obtained when $CoK\alpha$ and $CuK\alpha$ (Fig. 2b and 2c) were used showed that the $AlTi_3$-H appeared after 24 h charging (diffraction peaks from 200, 002, 201, 202, 203 and 421 planes of the $AlTi_3$-H phase appeared). $AlTi_3$-H has an expanded hcp structure with a lattice parameter of $a = 0.5865$ nm and $c = 0.4730$ nm, which is about 1.5% greater than that of original $AlTi_3$ matrix. Due to an overlap of $AlTi_3$-H and $AlTi_3$ reflections, the change in shape of diffraction peaks during ageing was rather complicated. Changes in line position and peak profile of $AlTi_3$-H and $AlTi_3$ in a Ti24Al–11Nb alloy after 24 h of cathodic charging, clearly show that as the hydrogen outgasses from the specimen there is a coexistence of a two-phase $AlTi_3$ and $AlTi_3$-H system in hydrogen charged aluminides, discontinuous transformations of $AlTi_3$ to $AlTi_3$-H during charging, and $AlTi_3$-H to $AlTi_3$ transformation during the ageing.

The quantitative X-ray method [8] is aimed at the analysis of the hydride distribution in thin surface

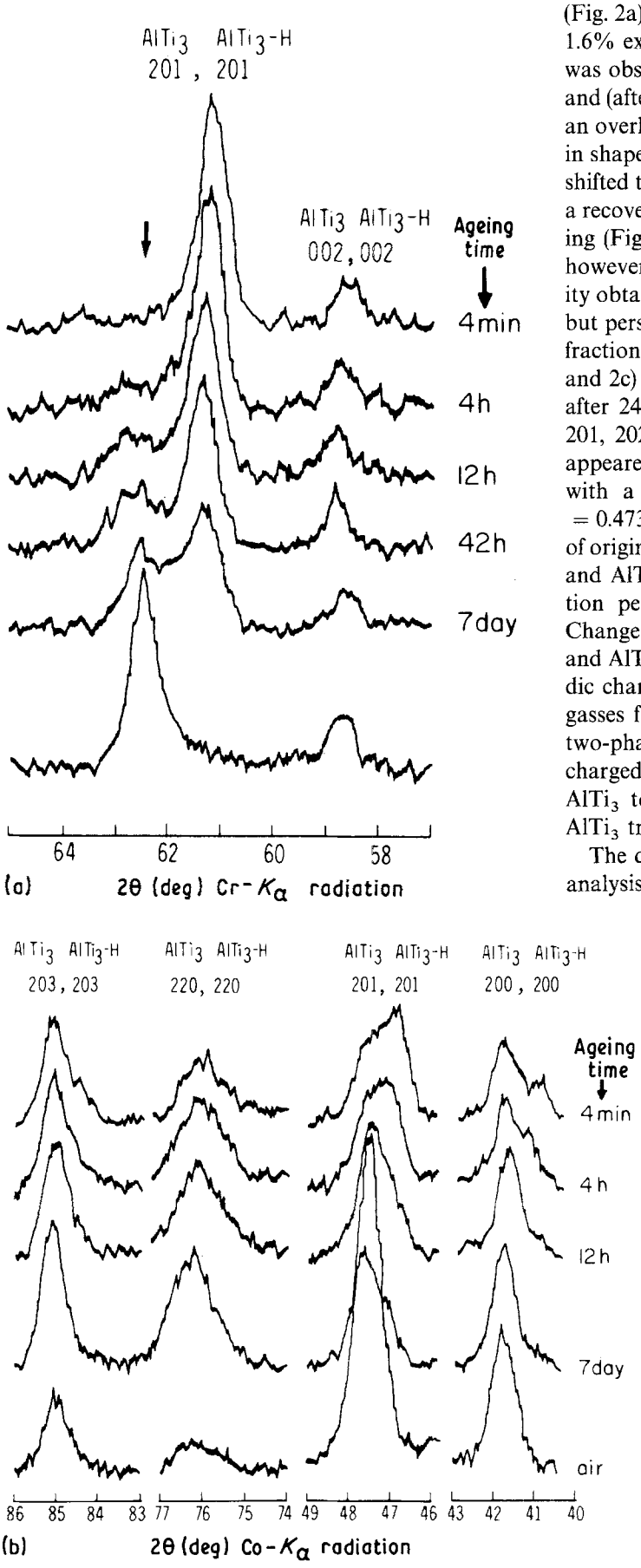

Figure 2 X-ray diffraction patterns after ageing times (24 h cathodically charged) for the times indicated of Ti–24Al–11Nb alloys (a) CrK_α radiation; (b) CoK_α radiation; (c) CuK_α radiation.

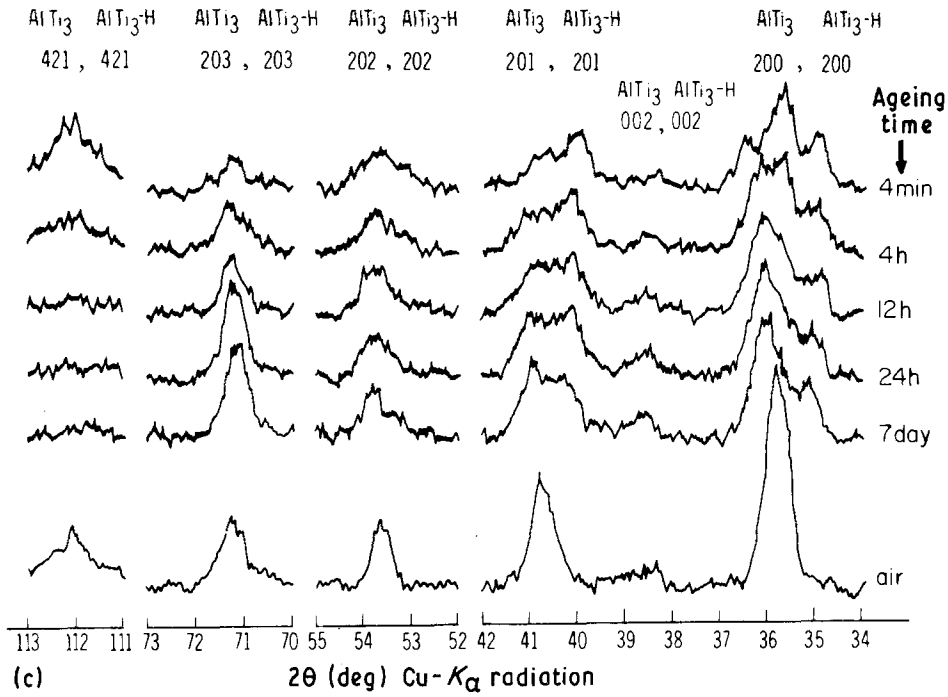

Figure 2 Continued

layers comparable to the penetration depth of the X-ray. The hydride distribution will be modelled mathematically, and the parameters of the distribution valued from diffraction data taken for various peaks and with various radiations. The distribution of the $AlTi_3$ matrix and $AlTi_3$-H hydride in the surface layer of the alloy is determined by

$$\frac{I_{AlTi_3 j}}{I_{0\,AlTi_3 j}} = C_{0\,AlTi_3} + \frac{1 - C_{0\,AlTi_3}}{x_0} \frac{\sin \theta_{AlTi_3}}{2\mu} \times [1 - \exp(-2\mu x_0 / \sin \theta_{AlTi_3})] \quad (1)$$

where j is the number of the diffraction peak, μ the mean linear attenuation coefficient, $\theta_{AlTi_3 j}$ the Bragg angle, $I_{AlTi_3 j}$ the intensity of the $AlTi_3$ diffraction peak, I_{0AlTi_3} the intensity for the pure matrix ($AlTi_3$) diffraction peak, and x_0 the phase definite depth on the surface of the specimen. The integral intensities of the $AlTi_3$ peak 200, 201, 202, 203 were measured using $K\alpha$ radiations from copper, cobalt and chromium. The best parameters C_{0AlTi_3} and x_0 were found by minimization of the sum

$$\sum_{j=1}^{N} [(I_j/I_{0j})_{calc} - (I_j/I_{0j})_{obs}]^2 \quad (2)$$

where $(I_j/I_{0j})_{calc}$ is calculated according to Equation 1, $(I_j/I_{0j})_{obs}$ are the observed values, and N the number of measurements with various θ_{AlTi_3}/μ values.

Calculated relation intensity curves and experimental data of the alloy which has been cathodically charged for 24 h, and aged for 4 h and 7 days, are shown in Fig. 3a and 3b. The most suitable parameters were found to be $C_{0AlTi_3} = 0.3$, $C_{0AlTi_3\text{-}H} = 0.7$ and $C_{0AlTi_3} = 0.36$, $C_{0AlTi_3\text{-}H} = 0.64$, for 4 h and 7 day aged alloys, respectively. The mean square deviation of the $(I_j/I_{0j})_{obs}$ from these parameters is equal to 0.0125 when $x_0 = 2$ μm. The weight fraction value of the $AlTi_3$-H, $C_{0AlTi_3\text{-}H}$ was found from the relation

$$C_{0AlTi_3} + C_{0AlTi_3\text{-}H} = 1 \quad (3)$$

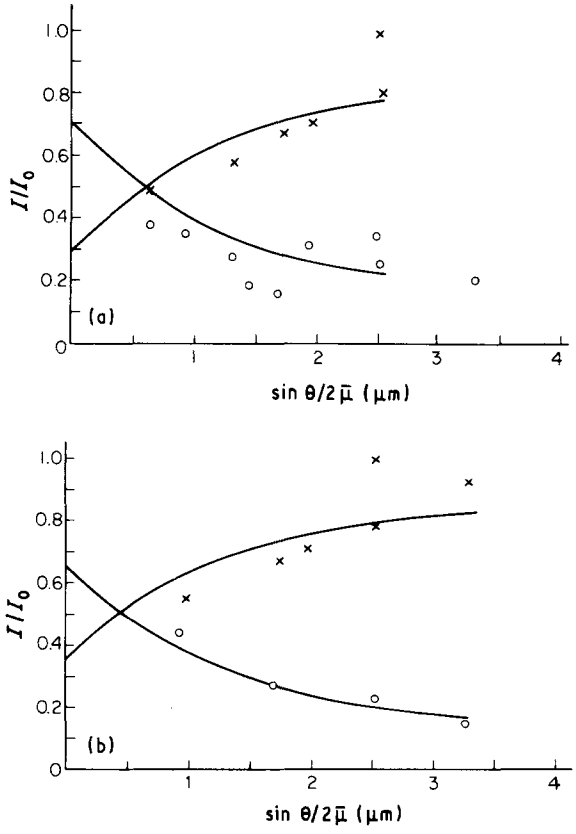

Figure 3 Calculated relative intensity curves and experimental data (24 h cathodic charged): (a) after 4 h ageing, (b) after 7 day ageing. (○ hydride, × $AlTi_3$, — calculated)

The distribution of the retained $AlTi_3$ matrix and $AlTi_3$-H in the surface layer of the alloy after charging for 24 h and after 4 h and 7 day ageing is shown in Fig. 4a and 4b, respectively. For samples aged for 4 h, the fraction of $AlTi_3$-H drops from about 70% on the surface to zero at a depth of approximately 2 μm. The amount of $AlTi_3$-H in this type of alloy decreased after a long (7 days) period of ageing to about 64% on the

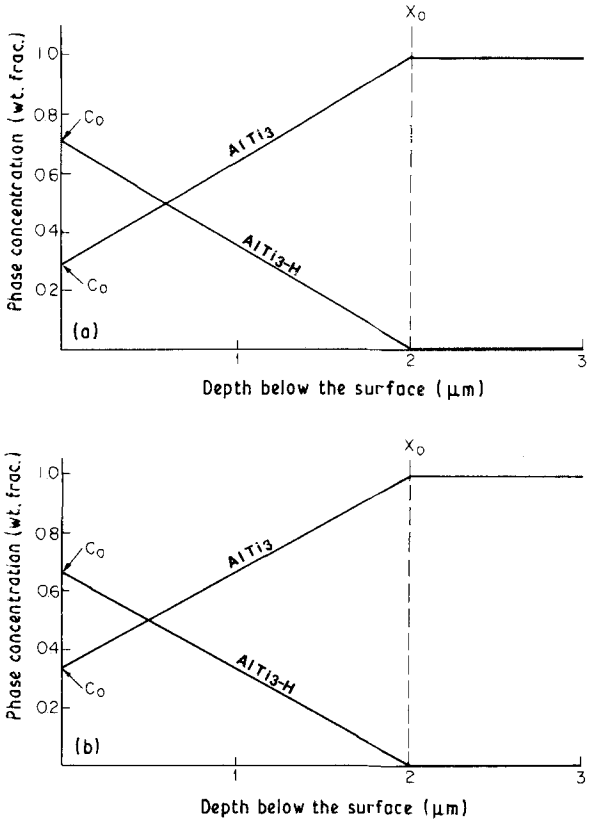

Figure 4 Phase distribution in surface layers in Ti–24Al–11Nb alloys cathodically charged (24 h): (a) after 4 h ageing, (b) after 7 day ageing.

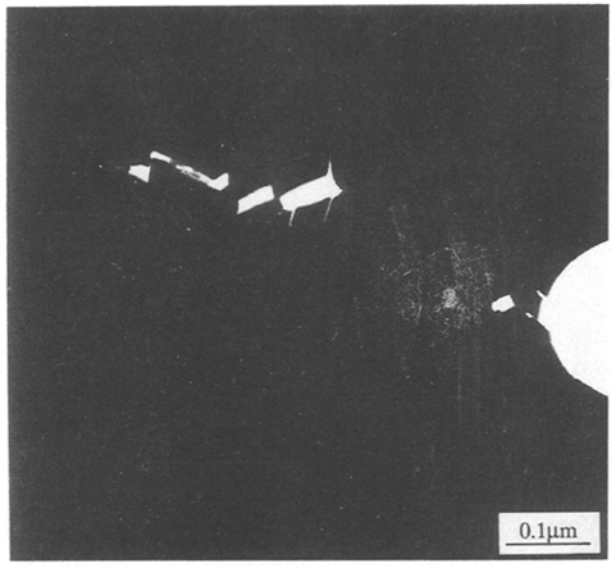

Figure 5. TEM micrographs in the mesh-image magnification showing the specimen hole in the Ti–24Al–11Nb alloy, and cracks which were formed after cathodic hydrogen charging at the hole edge zones.

surface, and drops to zero at a depth of approximately 2 μm.

Fig. 5 represents the formation of cracks induced by hydrogen charging in this alloy. TEM micrographs in the small magnification show cracks which were formed by cathodic charging at the hole edge. The experimental results indicate that hydrogen induced main transgranular cracks and microcracks among the needles of the "acicular" microstructure were found.

Diffraction peak shifts, line broadening, and the appearance of new reflections were observed in this study after hydrogen charging and during outgassing after charging (Figs 1 and 2). Hydrogen penetration considerably expands the lattice of $AlTi_3$ matrix, and causes a greater shift in diffraction peak towards the lower 2θ angles. Hydrogen penetration causes broadening of the $AlTi_3$ phase, which also decreases with time of ageing, when hydrogen is outgassed from the specimen (Fig. 1). In the uniform solid solution, the intensity of the diffraction peaks decreases due to local lattice distortion, but the peaks themselves remain sharp. The reason for peak broadening in our case seems to be the formation of a non-uniform solid solution of hydrogen in the $AlTi_3$ matrix. Hydrogen penetration during charging and hydrogen release during ageing are diffusion controlled, and large concentration gradients in the thin surface comparable with the depth of X-ray penetration are expected. Actually, the hydrogen concentration is non-uniform within the thin surface layers. The non-uniform concentration of hydrogen results in non-uniform expansion of the material. The latter inevitably leads to the development of the internal stresses.

Hydrides having several variants were formed in the stress field and hydrogen environments. In the Ti-H system two types of hydride phases have been known to exist, the δ and ε hydrides. The δ hydride has an fcc structure of CaF_2 type in which hydrogen atoms occupy tetrahedral sites randomly, having a wide range of non-stochiometric composition $TiH_{1.5}$–$TiH_{1.99}$. At higher concentrations near TiH_2, the ε hydride, being fct with $c/a < 1$ appears at low temperatures [9–11]. Other δ hydrides (fct structure, $c/a = 1.09$ and $c/a = 1.12$), which were formed in the α phase matrix in titanium at low concentrations 1–3 at %, have been reported [12, 13]. The present observation shows an $AlTi_3$-H hydride transformation induced by cathodic charging of Ti–24Al–11Nb alloys, which suggests that both the hydrogen concentration and stress state in the near-surface region must be considered to play a significant role. As shown in Figs 1 and 2, significant transformation of $AlTi_3$ to $AlTi_3$-H occurred during charging of the alloy. The *d*-spacing obtained from $AlTi_3$-H was found to be very similar to $TiH_{1.96}$ or ε hydrides [9–13]. However, only $AlTi_3$-H is consistent with all diffraction peak behaviour in this study. Existence of other hydride phases, probably based on the Ti–Nb–H composition, is possible too. The $AlTi_3$-H hydride peaks should be distinct from coexisting peaks of the $AlTi_3$ matrix whose lattice parameter is also increased by dissolved hydrogen. The peak intensity and lattice parameter variations of $AlTi_3$ and $AlTi_3$-H phases, during charging and aging (Fig. 2), are consistent with a two-phase region with a miscibility gap between them. Under the high fugacity condition present during cathodic charging, the $AlTi_3$ matrix is first enriched with hydrogen until concentration is exceeded at which time $AlTi_3$-H phase composition C_{crit} (critical hydrogen concentration for hydride formation) is able to form. The interface between $AlTi_3$

and $AlTi_3$-H moves inward under the surface, and the $AlTi_3$-H at the surface is then enriched with hydrogen up to a concentration higher than C_{crit}. The reason for the variation in the $AlTi_3$ and $AlTi_3$-H peak intensities and lattice parameters is the X-ray measurement obtained from thin surface layers of the material, which is average over the hydrogenated volume and radiation penetration. Upon outgassing, this $AlTi_3$-H region loses hydrogen rapidly until its hydrogen concentration decreases to C_{crit}. Further loss of hydrogen does not decrease the $AlTi_3$-H lattice parameter, but does decrease the amount of $AlTi_3$-H phase, as observed in Fig. 2. Only when $AlTi_3$-H is completely gone does the lattice parameter of the $AlTi_3$ decrease, which is to be expected after a long period of ageing.

In general a metal hydride has a larger specific volume than a host metal so that nucleation of hydride is accompanied by misfit strain. The magnitudes for this strain misfit were between 15 and 20% for formation of hydrides in α phase [9]. $AlTi_3$ specimens revealed extensive bending after cathodic charging (on one side) of the sample during a period of 12 h at room temperature. High interval tensile stresses developed on the outer surface, and compressive stresses on the non-treated side of the specimens. Nucleation and growth of hydrides takes place under the mechanical constraint of the matrix, therefore, the formation of the $AlTi_3$-H appears during cathodic charging of the Ti–24Al–11Nb alloy. The relaxation of tensile stresses can be possible by formation of cracks. Two fracture mechanisms in h c p α Ti–4Al wt % alloy [2] have been observed in a gaseous hydrogen environment at room temperature: one is fracture by localized plastic deformation enhanced by the presence of hydrogen, the other is a brittle fracture of the stress-induced titanium hydride which precipitates at elastic singularities. At high stress intensities the crack propagates by the process of hydrogen enhanced localized plasticity, while at low stress intensities titanium hydrides form in the vicinity of crack tips and crack propagation proceeds through the hydrides.

4. Conclusions

The conclusions are as follows.

(1) In cathodically charged Ti–24Al–11Nb alloy transformation of $AlTi_3$ matrix is probably to $AlTi_3$-H hydride and depends on the particular hydrogen distribution after the charging and during outgassing.

(2) The fraction of $AlTi_3$-H drops from about 70% on the surface to zero at a depth of approximately 2 μm for samples which were charged for 24 h and aged for 4 h. The weight fraction of the $AlTi_3$-H hydride in the surface decreased after a long period of ageing (7 day) to about 64%.

(3) Hydrogen induced cracking as a result of the cathodic charging in the absence of external stress.

References

1. M. F. RONALD, *Adv. Mater. Proces.* **135** (1985) 29.
2. D. S. SHIH, I. M. ROBERTSON and H. K. BIRNBAUM, *Acta Metall.* **36** (1988) 111.
3. D. S. SHIH and H. K. BIRNBAUM, *Scripta Metall.* **20** (1986) 1261.
4. H. NUMAKURA and M. KOIWA, *Acta Metall.* **32** (1989) 1977.
5. J. D. BOYD, *Trans. ASM* **62** (1969) 977.
6. H. P. KLUG and L. E. ALEXANDER, in "X-Ray Diffraction" (Wiley, New York, 1974) p. 360.
7. JCPDS 14-451 (Joint Committee on Powder Diffraction Standards, Swarthmore, Pennsylvania 1972)
8. L. S. ZEVIN, P. ROZENAK and D. ELIEZER, *J. Appl. Crystallogr.* **17** (1984) 18.
9. S. S. SILKE, L. BEALON and D. D. ZARBERIS, *Acta Crystallogr.* **9** (1956) 607.
10. H. L. YAKEL Jr., *ibid.* **11** (1958) 46.
11. P. MILLEBACH and M. GIVON, *J. Less-Common Met.* **87** (1982) 197.
12. H. NUMAKURA and M. KOIWA, *Acta Metall.* **32** (1984) 1799.
13. O. T. WOO and G. J. C. CARPENTER, *Scripta Metall.* **19** (1969) 977.

Received 4 October 1989
and accepted 9 April 1990